Carbon ion plume emission produced by charge exchange with neutral beams on National Spherical Torus Experiment

Ronald E. Bell
Princeton Plasma Physics Laboratory, Princeton University, Princeton, New Jersey 08543-0451

(Received 7 May 2006; presented on 9 May 2006; accepted 16 May 2006; published online 21 September 2006)

Emission from impurity ions excited by charge exchange with injected beam neutrals is widely used to provide local measurements of ion temperature, velocity, and density. Following the charge exchange process, hydrogenic impurity ions travel along magnetic field lines and may be excited by electron impact from the ground state before they are ionized, producing "plume" emission. This nonlocal emission from plume ions that drift into view can adversely affect the interpretation of charge exchange spectra. Carbon plume emission is observed in the background sightlines of the charge exchange recombination spectroscopy diagnostic of the National Spherical Torus Experiment. In plasmas with high rotation, superthermal flow of carbon ions produces a near Gaussian line shape for the plume emission. Modeling of the production, electron impact excitation, and ionization of the plume ions along the magnetic field lines yields line widths and line shifts consistent with observations. A radial shift between the measured and modeled plume brightness profiles is observed. Plume emission is observed on sightlines that equilibrium reconstruction indicates are not connected to the neutral beam volume, indicating a possible new constraint for the equilibrium reconstruction. © *2006 American Institute of Physics.* [DOI: 10.1063/1.2217012]

I. INTRODUCTION

Charge exchange recombination spectroscopy has long been an important diagnostic tool for high temperature plasmas with neutral beam injection.[1] Profiles of ion temperature, plasma velocity, and impurity concentration provide critical input for the study of thermal and particle transport. A fully ionized impurity ion can capture an electron by charge exchange with a fast beam neutral, leaving it in an excited state. The excited hydrogenic impurity ion will promptly emit a photon providing a localized measurement. Nonlocal emission from the plasma edge at the same wavelength will also contribute to the observed signal on a line-integrating viewing chord. After the charge exchange process, it is possible for the product impurity ion in the ground state to be reexcited by electron impact, and emit again before ionization producing "plume" emission.[2] This name refers to the nonlocal emission that can arise as parallel transport allows these plume ions to drift into view from portions of the beam volume away from the line of sight, contaminating the spectrum with emission having a different linewidth and wavelength shift. Modulation of the neutral beam source is often used to eliminate the contributions from nonlocal edge emission, but modulation is ineffective for eliminating plume emission, since it is prompt with the neutral beam. The observed plume spectra distinguish positive and negative parallel velocity components in the ion's velocity distribution, which will take different paths around the torus with different attenuation. The spectral profile for plume emission is distorted when only a portion of the velocity distribution is observed. Plume emission is especially important for low Z impurities such as helium,[3,4] where for visible lines, it can be comparable to the charge exchange (CX) emission. Plume emission from higher Z impurities, such as carbon, is often assumed negligible due to the higher excitation energies necessary for the higher n-level transitions.[3,5]

After charge exchange, a carbon ion in the $n=8$ level will emit a photon in $\sim 10^{-9}$ s. Even with a toroidal plasma velocity of ~ 250 km/s, typical for National Spherical Torus Experiment (NSTX), this results in very good localization. Ionization times for the plasmas considered here are $\sim 10^{-4}$ s, with ionization mean free paths of ~ 10 m, several times a toroidal circumference. Whether the plume emission can be observed depends on the balance of the relevant atomic rates, which will vary with plasma conditions, and viewing geometry. High plasma density can pair high plume ion production at larger radii against heavily attenuated charge exchange signals in the core with line-integrating sightlines.

Plume emission from carbon ions has been observed in the background sightlines of the charge exchange spectroscopy diagnostic of the NSTX. The plume emission is readily discernible in plasmas with high toroidal rotation, where emission from the fast plume ions in the core is shifted in wavelength from edge emission.

The purpose of this article is to examine and model the observed carbon plume emission in plasmas with high rotation where a good comparison can be made. The extent of the contribution of plume emission to the measured signal of other plasmas might then be revealed. The distorted spectral profile of plume emission for low or nonrotating plasmas might then be taken into account to improve the analysis of charge exchange spectroscopy data. Additionally, it is noted

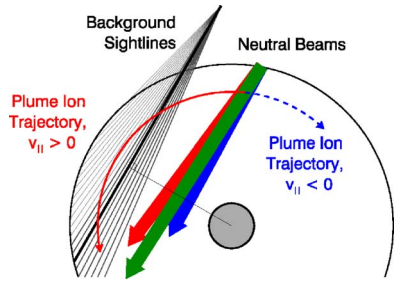

FIG. 1. (Color online) Background sightlines are oriented to view adjacent to neutral beam sources. A plume ion, born in the neutral beam volume, with parallel velocity may be observed where its path intersects a background sightline.

that observation of plume emission on magnetic field lines that pass near the edge of the neutral beam can place useful constraints on the local pitch angle.

II. MEASUREMENTS

The NSTX charge exchange recombination spectroscopy (CHERS) diagnostic uses the carbon $n=8-7$ transition at 5290.5 Å. A set of midplane sightlines, viewing the local charge exchange emission, intersects the neutral beams nearly tangent to the flux surfaces for good radial resolution. Background sightlines are used to measure the contribution due to edge emission with views adjacent to the three NSTX neutral beam sources; see Fig. 1. This article will examine the plume emission observed in these background sightlines.

NSTX is a spherical tokamak with a major radius of 85 cm. The NSTX plasma considered here had a plasma current of 750 kA, a toroidal magnetic field of 3.5 kG, and 6 MW of heating power supplied by three neutral beam sources operated at 90 kV using deuterium. The half width of the neutral beam in the plasma is 12.2 cm wide by 44 cm tall. Figure 2 shows kinetic profiles for shot 11 6313. In the lower panel, the toroidal velocity reaches 200 km/s, which is 1.6 times the carbon thermal velocity, and the low magnetic field in this geometry results in pitch angles up to 40°.

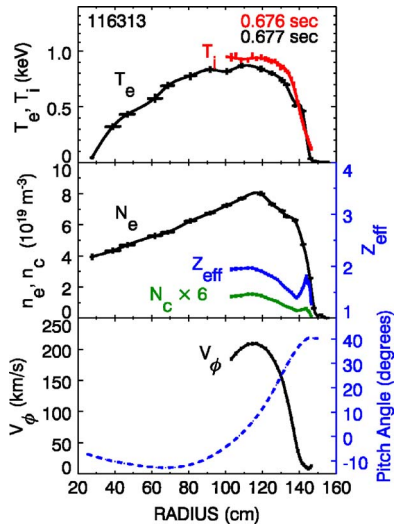

FIG. 2. (Color online) Measured temperature, density, rotation, and pitch angle profiles for shot 116 313 at 676 ms.

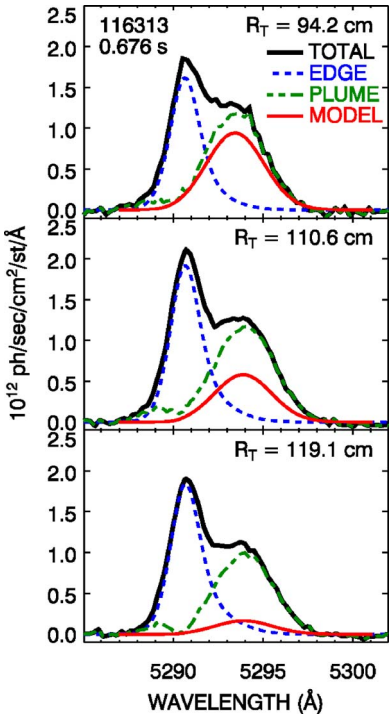

FIG. 3. (Color online) Spectra observed at different tangency radii. TOTAL refers to the measured spectrum. EDGE is a reconstruction of the brightness due to edge emission. PLUME is the inferred plume brightness obtained by subtracting the edge spectra from the full signal. MODEL is the modeled spectrum.

These last two features help the identification of plume emission in the background spectra. The wavelength shifted plume emission can be readily distinguished from the nearly unshifted edge emission. When the carbon plume ions exceed their thermal velocity, a near Gaussian line shape results, since nearly the entire velocity distribution has positive parallel velocity, $v_{||}$. The large pitch angles of the magnetic field lines serve to confine the observed plume emission to the core radii. Following the magnetic field lines, the plume ions can rise well above the midplane sightlines, and be out of view of the midplane background sightlines. Indeed, for the plasma considered here, there is no plume emission observed outside of major radius of 130 cm.

Figure 3 shows measured spectra in three of the background sightlines at three tangency radii (bold line). The background brightness profile outside of 130 cm was inverted to get local emission values for the edge brightness. This inverted emission profile and measured T_i and V_ϕ profiles are used to reconstruct the spectral contribution of the edge by summing emission weighted Gaussians with the proper local spectral width, and line shift and integrating over the viewing path. These spectral contributions are labeled EDGE and are shown as dashed profiles in Fig. 3. Subtracting the reconstructed edge profiles from the total signal gives an estimate of the brightness, width, and line shift of the plume contribution, which is quite similar to the line shapes of the CX emission seen at the active views. This profile appears to be near Gaussian, consistent with the superthermal flow expected in the core. Figure 4 shows the radial profiles of the measured plume brightness, the brightness due to the edge, and, for comparison, the CX brightness

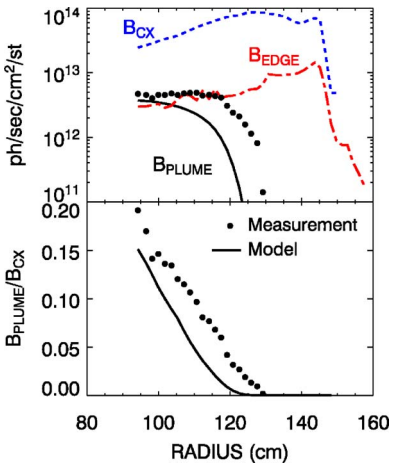

FIG. 4. (Color online) Radial profiles of measured brightnesses of C^{5+}. Top: B_{CX} (dotted) is the observed brightness in the active sightlines due to charge exchange emission. B_{EDGE} (dashed) is the reconstructed brightness due to edge emission. The plume brightness from measurement (circles) and model (solid) rivals edge brightness in core. Bottom: The measured and modeled ratios of plume to active CX emission are shifted by ~9 cm, indicating magnetic field lines near 125–130 cm connect to the neutral beam volume, though the equilibrium reconstruction indicates they fall below.

from the CHERS views of the neutral beams. The plume brightness for this discharge rivals the edge brightness in the core plasma, and can be up to 20% of the CX brightness for the innermost views.

III. MODELING

The plume modeling here generally follows the treatment of plume emission in Ref. 2. Here, however, the full magnetic field equilibrium reconstruction is used to map the path of a plume ion along the magnetic field line, and to map the midplane profile measurements into two dimensions. The full beam geometry is used to compute the beam footprint.[6] The neutral beam attenuation is computed in three dimension for accurate path integrals. Beam stopping cross sections are computed using a multistep ionization treatment found in Ref. 7, using updated coefficients to extend the relevant energy range of the beams. Midplane measurements of electron temperature, T_e, and electron density, n_e, are treated as flux functions. This is not strictly true for n_e, although it should be adequate for a mapping confined to outer midplane region. Excitation and ionization rates from electron impact are taken from Sampson and Zhang.[8] Total electron capture cross sections for carbon were taken from Janev *et al.*[9]

The brightness of the plume emission is an integral along the viewing chord,

$$B_{\lambda}^{\text{plume}} = \frac{1}{4\pi}\int n_e Q^{\text{ex}} n_{C5+}^{\text{cx}} b_{\lambda} d\ell, \tag{1}$$

where $Q^{\text{ex}}=Q^{\text{ex}}(T_e)$ is the excitation rate from the ground to the upper n level of the transition, n_{C5+}^{cx} is the density of the carbon plume ions, and b_{λ} is the branching ratio for the observed transition. The carbon plume ions are born in the beam volume, where without parallel transport a balance of the charge exchange and ionization rate yields,

$$\frac{n_{C5+}^{cx}}{n_{C6+}} = \frac{\sum_J n_j^b \langle \sigma\nu\rangle_j^{\text{tot}}}{n_e Q_{C5+}^{\text{ion}}}, \tag{2}$$

where n_{C6+} is the density of fully stripped carbon which will determined from charge exchange spectroscopy, n_j^b is the neutral density for the jth beam component (full, half, and third energies for deuterium beams), $\langle\sigma\nu\rangle_j^{\text{tot}}$ is the total CX cross section, and $Q_{C5+}^{\text{ion}}=Q_{C5+}^{\text{ion}}(T_e)$ is the ionization rate coefficient for C^{5+}. The total plume brightness is computed using an average density for the C^{5+} product ion along the intersecting path of a magnetic field line with the beam,

$$n_{C5+}^{\text{cx}}(S) = \frac{\xi(S)}{w}\int n_{C6+}\frac{\sum_J n_j^b \langle\sigma\nu\rangle_j^{\text{tot}}}{n_e Q_{C5+}^{\text{ion}}} ds, \tag{3}$$

where S is the distance along the flux tube, $\xi(S)$ is an attenuation coefficient to take into account ionization losses along the flux tube, and w is the nominal beam width. $\xi(S)$, which will vary along the flux tube, has been derived in Ref. 2 to preserve continuity around the torus. For positive going ions,

$$\xi_+(S) = \frac{2\sinh(d/\lambda_i)}{1-e^{-2L/\lambda_i}} e^{-S/\lambda_i} \tag{4}$$

for $d \leqslant S \leqslant L$, where d is the half width of the beam and L is half the length of the field line around the torus, and $\lambda_i = \nu_{\|}\tau_i$ is the ionization mean free path for particle with velocity $\nu_{\|}$. The ionization time is given by $\tau_i^{-1}=n_e Q_{C5+}^{\text{ion}}$. For the high rotation case, $\nu_{\|}$ was taken to be the toroidal velocity.

The magnetic field line path for points along each background sightline were mapped from the midplane to where they intersected the toroidal location of each neutral beam. The contributing beam density in the beam volume was determined using computed beam stopping cross sections and integrating over velocity space for the portion of the distribution with positive $\nu_{\|}$. Integrating through the beam volume using Eq. (3), an average plume ion density was computed. This density was attenuated using Eq. (4) to get local values along the sightline. The plume brightness was computed by integrating along the path of the sightline. The spectral profile was obtained in a similar fashion, but the integral over velocity space was only performed in the two dimensions perpendicular to the direction of view of the background sightline.

IV. RESULTS

The modeled spectral profiles shown in Fig. 3 agree well in line shape and wavelength shift with the observed plume emission. The modeled amplitude is less than the measured value with the discrepancy increasing with radius. This is also clear from the modeled brightness profile in Fig. 4. This modeling shows, using standard atomic rates, that plume emission should be expected to be observed in these plasmas, and that the spectral profiles are representative of those observed in these high rotating discharges. With brightness comparable to background brightness from the edge, it is

necessary to account for this nonlocal emission, which is more difficult for plasmas with low rotation, to ensure accurate T_i, V_ϕ, and n_c measurements.

The ratio of plume brightness to the brightness of the CX emission shows a radial shift of ~9 cm between the modeled and measured values. Note that for $R_T > 125$ cm, the modeled brightness is essentially zero, while there is still a measurable plume signal. An observation of a finite plume signal indicates that there is a magnetic field line that connects that sightline to the neutral beam volume. The modeled brightness is zero simply because the magnetic field lines are computed from the equilibrium reconstruction to miss the neutral beam, in this case to pass under the beam, rather than from any details of the atomic physics. This inconsistency might result from a neutral beam footprint that is taller than used in the modeling, cross-field transport of the impurity ions, or an incorrect pitch angle between the midplane and the bottom of the neutral beam. The height of the beam, characterized in Ref. 6, is consistent with the damage pattern seen on the graphite tiles of the neutral beam armor on the opposite side of the torus. Cross-field transport would imply a movement of many centimeters over about a 1 m path as the magnetic field line traverses about a 60° angle between the neutral beam and the sightline. The equilibria have been constrained with internal pitch angle measurements from a motional Stark effect diagnostic on the midplane, and take into account centrifugal forces due to the toroidal velocity.[10] The measurement of the plume brightness might add another constraint on the vertical extent of the current distribution in the beam.

ACKNOWLEDGMENTS

This work has benefited from useful discussions with E. J. Synakowski. The author would also like to thank J. E. Menard and S. A. Sabbagh for equilibrium reconstructions and B. P. LeBlanc for Thomson scattering profiles. This work was supported by DOE Contract No. DE-AC02-76-CH0307.

[1] R. C. Isler, Plasma Phys. Controlled Fusion **36**, 171 (1994).
[2] R. J. Fonck, D. S. Darrow, and K. P. Jaehnig, Phys. Rev. A **29**, 3288 (1984).
[3] E. J. Synakowski *et al.*, Phys. Rev. Lett. **75**, 3689 (1995).
[4] U. Gerstel, L. Horton, H. P. Summers, M. von Hellermann, and B. Wolle, Plasma Phys. Controlled Fusion **39**, 737 (1997).
[5] W. P. West *et al.*, Phys. Plasmas **9**, 1970 (2002).
[6] J. H. Kamperschroer, L. R. Grisham, N. Kokatnur, L. J. Lagin, R. A. Newman, T. EH. O'Connor, T. N. Stevenson, and A. von Halle, Rev. Sci. Instrum. **66**, 130 (1995).
[7] C. D. Boley, R. K. Janev, and D. E. Post, Phys. Rev. Lett. **52**, 534 (1984).
[8] D. H. Sampson and H. L. Zhang, Astrophys. J. **335**, 516 (1998).
[9] R. K. Janev, R. A. Phaneuf, and H. T. Turner, At. Data Nucl. Data Tables **40**, 249 (1988).
[10] S. A. Sabbagh, A. C. Sontag, and J. M. Bialek, Nucl. Fusion **46**, 635 (2006).